

RESEARCH

Open Access



Selective block of sensory neuronal T-type/ Cav3.2 activity mitigates neuropathic pain behavior in a rat model of osteoarthritis pain

Brandon Itson-Zoske^{1†}, Seung Min Shin^{1†}, Hao Xu^{1,2}, Chensheng Qiu^{1,2}, Fan Fan³, Quinn H. Hogan¹ and Hongwei Yu^{1*}

Abstract

Background: Peripheral and central nociceptive sensitization is a critical pathogenetic component in osteoarthritis (OA) chronic pain. T-type calcium channel 3.2 (Ca_v3.2) regulates neuronal excitability and plays important roles in pain processing. We previously identified that enhanced T-type/Ca_v3.2 activity in the primary sensory neurons (PSNs) of dorsal root ganglia (DRG) is associated with neuropathic pain behavior in a rat model of monosodium iodoacetate (MIA)-induced knee OA. PSN-specific T-type/Ca_v3.2 may therefore represent an important mediator in OA painful neuropathy. Here, we test the hypothesis that the T-type/Ca_v3.2 channels in PSNs can be rationally targeted for pain relief in MIA-OA.

Methods: MIA model of knee OA was induced in male and female rats by a single injection of 2 mg MIA into intra-knee articular cavity. Two weeks after induction of knee MIA-OA pain, recombinant adeno-associated viruses (AAV)-encoding potent Ca_v3.2 inhibitory peptide aptamer 2 (Ca_v3.2iPA2) that have been characterized in our previous study were delivered into the ipsilateral lumbar 4/5 DRG. Effectiveness of DRG-Ca_v3.2iPA2 treatment on evoked (mechanical and thermal) and spontaneous (conditioned place preference) pain behavior, as well as weight-bearing asymmetry measured by Incapacitance tester, in the arthritic limbs of MIA rats were evaluated. AAV-mediated transgene expression in DRG was determined by immunohistochemistry.

Results: AAV-mediated expression of Ca_v3.2iPA2 selective in the DRG-PSNs produced significant and comparable mitigations of evoked and spontaneous pain behavior, as well as normalization of weight-bearing asymmetry in both male and female MIA-OA rats. Analgesia of DRG-AAV-Ca_v3.2iPA1, another potent Ca_v3.2 inhibitory peptide, was also observed. Whole-cell current-clamp recordings showed that AAV-mediated Ca_v3.2iPA2 expression normalized hyperexcitability of the PSNs dissociated from the DRG of MIA animals, suggesting that Ca_v3.2iPA2 attenuated pain behavior by reversing MIA-induced neuronal hyperexcitability.

Conclusions: Together, our results add therapeutic support that T-type/Ca_v3.2 in primary sensory pathways contributes to MIA-OA pain pathogenesis and that Ca_v3.2iPAs are promising analgesic leads that, combined with AAV-targeted delivery in anatomically segmental sensory ganglia, have the potential for further development as a peripheral

[†]Brandon Itson-Zoske and Seung Min Shin contributed equally to this work.

*Correspondence: hyu@mcw.edu

¹ Department of Anesthesiology, Medical College of Wisconsin, Milwaukee, WI 53226, USA

Full list of author information is available at the end of the article



selective T-type/ $\text{Ca}_v3.2$ -targeting strategy in mitigating chronic MIA-OA pain behavior. Validation of the therapeutic potential of this strategy in other OA models may be valuable in future study.

Keywords: Monosodium iodoacetate, Osteoarthritis, Chronic pain, Dorsal root ganglia, Primary sensory neuron, T-type/ $\text{Ca}_v3.2$ channels, Adeno-associated virus

Background

Injection of monosodium iodoacetate (MIA), an inhibitor of glycolysis, into the intra-articular cavity of knee is an established preclinical OA pain model [1]. The pain pathogenesis in MIA-OA has been described as a multifaceted and time-dependent interrelated pathological processes, involving joint damage, structural reorganization of joint afferents, low-grade inflammation, and nerve damage-induced painful neuroplasticity, all contributing to the MIA-OA pain [2].

Ample evidence demonstrates that peripheral and central nociceptive sensitization plays crucial roles in the pathogenesis of OA pain. MIA-OA exhibits PSN and spinal dorsal horn (SDH) neuronal sensitization that resembles neuropathic pain conditions, suggesting mechanistic overlap in these two pathologies [3]. Many studies focus on changes in knee nociceptors and their sensitivity and summate that OA pain is generated and maintained through continuous distinct peripheral nociceptive inputs from the affected joint to their innervating PSNs in DRG [3]. These mechanisms include sensitization of joint afferents by local inflammation and release of inflammatory mediators, bone marrow lesions or micro fractures, subchondral bone remodeling, and increased intra-osseous pressure [4]. However, clinical observation of OA suggest widespread nociceptive sensitization that includes joint afferents and PSNs innervating tissues outside the arthritic joint. For example, most OA patients experience not only pain from the OA joint but also referred pain from the areas remote from the arthritic joint, such that pain severity in OA patients often fails to correlate with the degree of joint pathology [5]. Clinical findings also show that neuropathic pain feature is prevalent in patients with advanced hip and knee OA [6–8], and approximately 20% of patients continue to experience chronic pain after total knee arthroplasty [9]. Recent studies indicate that, in addition to joint damage, DRG-PSN somata morbidity and plasticity contribute to persistent OA neuropathic pain feature [2, 10].

MIA produces peripheral nerve injury responses with PSN somata damage as time progresses [11]. This leads to the dysfunction of peripheral sensory pathways in OA pain beyond exclusive sensitization of joint afferents and associated innervating PSNs [12], and adjacent non-joint innervating PSNs including C-, $\text{A}\delta$ -, and $\text{A}\beta$ -neurons are also extensively affected, which could induce

sensitization of affected joint, dermatomes, and increased nociceptive input to SDH [12, 13]. These comorbidities of joint- and non-joint-innervating PSN sensitization are recognized as an essential pathology for the development and maintenance of OA neuropathic pain-like behavior. Importantly, joint-MIA induced DRG inflammatory and neuronal pathology can maintain pain independent from the damage in the joint in the late pathological stage [14, 15], which may significantly influence the disease course.

Many PSN nociceptive molecules, e.g., voltage-gated ion channels [16, 17], are sensitized in MIA-OA. T-type/ $\text{Ca}_v3.2$ channels ($\text{Ca}_v3.2$), which are abundantly expressed in PSNs and their axons, determine low-threshold mechanoreceptor function, shape neuronal firing properties, and have been demonstrated in modulating chronic peripheral and central sensitization in various chronic pain conditions [18]. $\text{Ca}_v3.2$ knock-out reduces load-induced OA in mice [19]. Knee MIA induces elevated expression and enhanced function of PSN T-type/ $\text{Ca}_v3.2$ channels [16]. Here, we tested whether reversing enhanced T-type/ $\text{Ca}_v3.2$ channels selectively in DRG-PSNs will mitigate OA pain behavior. We generated AAV-encoding $\text{Ca}_v3.2$ inhibitory peptide aptamers ($\text{Ca}_v3.2\text{iPA}2$ and 1) that show selective and potent inhibition of $\text{Ca}_v3.2$ current without affecting ion channel gating properties in our prior studies [20]. Here, we showed that AAV-mediated selective expression of $\text{Ca}_v3.2\text{iPAs}$ in the PSNs in vivo produced significant attenuation of evoked and spontaneous pain behavior in both male and female MIA-OA rats. Hyperexcitability of PSNs in MIA rats was normalized after treatment, suggesting that $\text{Ca}_v3.2\text{iPA}$ attenuated pain by reversing injury-induced sensory neuronal hypersensitivity.

Methods

Animals

Experiments were performed in adult male and female Sprague Dawley rats (5–6 weeks old; 125–150 g body weight) purchased from Charles River Laboratories (Wilmington, MA, USA). Rats were housed in standard 12-h cycle lighting and were allowed ad libitum access to food and water prior to and throughout the experimental protocol. All animal experiments were performed with the approval of the Medical College of Wisconsin Institutional Animal Care and Use Committee in accordance with the National Institutes of

Health Guidelines for the Care and Use of Laboratory Animals. All efforts were made to minimize suffering and the numbers of animals used. All survival surgeries were completed in a sterile environment under a surgical microscope in animals anesthetized with isoflurane (2–5%). For tissue harvest euthanasia, animals were deeply anesthetized using isoflurane followed by decapitation with a well-maintained guillotine. The estimated numbers of animals needed were derived from our previous experience with similar experiments [16, 20], and a power analysis was not performed. The numbers of rats used were detailed in the relevant sections or figure legends of the experiments.

Induction of knee OA

The MIA model of knee OA was induced in isoflurane-anesthetized animals as previously described [21]. After briefly anesthetized with isoflurane (2% v/v) vaporized in oxygen, rats received a single intra-articular cavity injection of 2 mg MIA (Sigma-Aldrich, St. Louis, MO, USA) in 50- μ l sterile 1 \times phosphate-buffered saline (saline) delivered by a Hamilton syringe (7645-01, Thermo Fisher, Waltham, MA, USA) through the infrapatellar ligament of the right knee, assisted by flexed the knee at a 90° angle. Control rats received intra-articular injection of saline (50 μ l).

Behavior tests

Behavioral tests were conducted between 9:00 AM and 12:00 AM. Experimenters were blinded to the treatment. Animals were habituated in individual test compartments for at least 1 h before each testing [22, 23].

Evoked sensory behavior testing

Mechanical allodynia (von Frey (vF)) The threshold for withdrawing from normally innocuous mechanical stimulation was assessed by applying the calibrated monofilaments (Patterson Medical, Bolingbrook, IL, USA) to the plantar surface of the hindpaw. Briefly, animals were placed in Plexiglas® boxes on a grid surface to allow filament access to the hindpaw. Beginning with the 2.8-g filament, filaments were applied with just enough force to bend the fiber and held for 1 s. If a response was observed, the next smaller filament was applied, and if no response was observed, the next larger was applied, until a reversal occurred, defined as a withdrawal after a previous lack of withdrawal, or vice versa. Following a reversal event, four more stimulations were performed following the same pattern. The forces of the filaments before and

after the reversal, and the four filaments applied following the reversal, were used to calculate the 50% withdrawal threshold [24]. Rats not responding to any filament were assigned a score of 25 g.

Mechanical hyperalgesia Noxious punctate mechanical stimulation (pin test) was performed using the point of a 22-G spinal anesthesia needle that was applied to the center of the hindpaw with enough force to indent the skin but not puncture it. Five applications were separated by at least 10 s, which was repeated after 2 min, for a total of 10 touches. For each application, the evoked behavior was either a very brisk, simple withdrawal with immediate return of the foot to the cage floor, or a sustained elevation with grooming that included licking, chewing, and possibly shaking, which lasted at least 1 s. This latter behavior was referred to as a hyperalgesic response, which is specifically associated with place avoidance [25]. Hyperalgesia was quantified by tabulating hyperalgesia responses as a percentage of total touches.

Cooling stimulation (cold) Acetone was expelled from a syringe attached to PE220 tubing to make a meniscus that was touched to the plantar surface of the hindpaw, such that the drop spread out on the plantar surface of the paw without contact of the tubing to the skin. Each hindpaw was tested 3 times in alternating fashion. Any withdrawal was considered a positive response.

Heating plantar test (heat) Heat threshold of the hindpaw was determined using a Hargreaves device designed for the purpose of identifying thermal sensitivity (Paw Thermal Stimulator System, University Anesthesia Research & Development Group, San Diego, CA, USA). Rats were placed on a temperature-regulated glass platform heated to 30 °C and the hindpaws stimulated with a radiant heat source (50 W halogen bulb) directed through an aperture. The time elapsed from initiation of the stimulus until withdrawal (withdrawal latency) as measured by a series of photocells was measured. Each hind paw was tested 4 times and the withdrawal latency values averaged.

Gabapentin injection Gabapentin (GBP, Sigma-Aldrich) was dissolved in saline immediately before injections and administered intraperitoneally (i.p.) at a volume of 0.5–1.0 ml (final dose of 100 mg/kg body weight). The hindpaw vF and pin tests on the side of ipsilateral to MIA injection were performed at 15-min intervals for 3 h after GBP injection.

Spontaneous pain behavior testing

Conditioned place preference (CPP) The presence of spontaneous, ongoing aversiveness (i.e., affective dimension of spontaneous pain) was determined by GBP (i.p.)-induced CPP test, as we have previously described [20, 26] with minor modifications. This employs the strategy that the aversive affective dimension of spontaneous pain can be identified by the place conditioning effect of an analgesic administered in a recognizable location. A 3-chamber CPP apparatus was used (Med Associates, St. Albans, VT, USA) in which 2 sliding doors separate the central chamber from the 2 side chambers that have distinct wall stripes and flooring. Animal movement and times spent in each chamber were measured by computer-interfaced infrared photo beams. The CPP procedure consisted of the following phases: (1) On the pre-conditioning day, rats were allowed to explore both sides of chambers for 15 min, and the time spent on each side was recorded, and the preferred and nonpreferred chambers were identified. The animals showed an extreme pre-determined level of preference for one chamber ($\geq 70\%$ of total time) at this stage and were excluded for further study. (2) On the conditioning days, place conditioning was conducted using a biased assignment approach to drug pairing, in which saline was paired with the preferred chamber in the morning, and GBP was paired with the non-preferred chamber in the afternoon with a 6-h interval (injections were never paired with the middle grey chamber). Conditioning consisted of intraperitoneal injection and subsequent restriction of the animals within the non-preferred chamber for 45 min. We used a 45-min conditioning time on the basis of tests that GBP (i.p.) maximally reduced mechanical hypersensitivity at 30–60 min after injection. Animals were conditioned for 2 days since 2-day GBP has been reported sufficient to produce CPP in rodent pain model [27–30]. (3) For post-conditioning testing, the animals were placed back into the middle grey chamber of the CPP chambers with free access to all chambers for 15 min. The difference score for each animal was calculated, by subtracting the time spent in the saline-paired or GBP-paired chamber before pairing (during preconditioning) from the time spent in each chamber after pairing (postconditioning), and then averaged within each group. Each rat had only a single CPP test 6 weeks after AAV injection. A CPP effect is defined if the animals spend significantly more time in the GBP-paired chamber versus the saline-paired compartment.

Weight-bearing asymmetry (Wb) An Incapacitance tester (Columbus Instruments, Columbus, OH, USA) was used to determine hindpaw weight distribution as previously reported [16]. Rats were placed in an angled

Plexiglas chamber so that each hindpaw rested on a separate force plate. The change in hindpaw weight distribution was automatically calculated by the Incapacitance tester (the difference in the amount of weight (g) between the left and right limbs). Essentially, the apparatus calculates an average hindpaw weight distribution over the span of 5 s, and three recordings are taken for each rat. All three recordings are then automatically averaged, and a mean score is displayed. The primary dependent measure was % weight on ipsilateral hindpaw and was determined by the formula: $\text{weight bearings (\%)} = \frac{\text{force (g) of right hindpaw}}{\text{force (g) of left hindpaw} + \text{force (g) of right hindpaw}} \times 100$. A value of less than 50% indicates a reduction in weight borne on the ipsilateral hindlimb.

AAV constructs

Production, purification, and titration of AAV constructs, including AAV6-GFPCav3.2iPA1 (AAV6-3.2iPA1), AAV6-GFPCav3.2iPA2 (AAV6-3.2iPA2), and AAV6-GFPCav3.2NP (AAV6-NP, inert Cav3.2 peptide from protein N-terminus as control), have been described previously [20]. The titers (GC/ml) of AAV6-3.2iPA1, 2, and AAV6-NP vectors were 2.45×10^{13} , 3.05×10^{13} , and 2.26×10^{13} , respectively. One lot of viral preparation for each vector was used for in vivo experiments.

Microinjection of AAV vectors into DRG

AAV vector solution was microinjected into the right lumbar (L) 4 and L5 DRG using previously described techniques [22]. Briefly, the surgically exposed intervertebral foramen was slightly enlarged by the removal of laminar bone. Injection was performed through a micropipette that was advanced $\sim 100 \mu\text{m}$ into the ganglion. Rats received L4 and L5 DRG injections of either AAV6-3.2iPA or AAV6-3.2NP (one vector per rat), consisting of $2 \mu\text{l}$ with adjusted titers containing a total of 2.0×10^{10} genome viral particles for each DRG. Injection was performed over a 5-min period using a microprocessor-controlled injector (Nanoliter 2000, World Precision Instruments, Sarasota, FL, USA). Removal of the pipette was delayed for an additional 5 min to minimize the extrusion of the injectate. Following the injection and closure of overlying muscle and skin, the animals were returned to their housing where they remained as the designed experiments required.

Histology and immunohistochemistry

Knee histopathological analysis

The knee joints from the tibia to the distal metatarsal including the tarsal joint were resected and fixed with 10% neutral-buffered formalin for 1 week at room temperature. The fixed specimens were decalcified in

Immunocal (Thermo Fisher) for 2 weeks and embedded in paraffin. Sagittal sections of the knee specimens were acquired from the paraffin blocks at 10 μm thickness, deparaffinized, and rehydrated in the order of xylene and series of absolute to 50% alcohol. The rehydrated sections were stained with hematoxylin and eosin (H&E), as described previously [16], for the observation of morphological changes in the articular tissues. Images of knee joint histology were captured using a Keyence BZ-X800 microscope (Keyence Corporation, Itasca, IL, USA).

IHC

Our previously described protocol was adopted [20]. In brief, the formalin-fixed, paraffin-embedded (FFPE) tissue sections were deparaffinized, hydrated, and treated by heat-induced antigen epitope retrieval in 10 mM citrate buffer, pH 6.0. Non-specific binding was reduced by incubating the sections for 30 min with a solution of 5% BSA in PBS plus 0.05% Tween20 (PBST). Samples were first immunolabeled with the selected primary antibodies (GFP 1:100, $\text{Ca}_v3.2$ 1:100, CGRP 1:100, and GFAP 1:1000, all described previously) [20] in a humid atmosphere overnight at 4 °C. All antibodies were diluted in PBST, containing 0.05% Triton X-100 and 5% bovine serum albumin (BSA). Normal immunoglobulin G (IgG from the same species as the first antibody) was replaced for the first antibody as the negative controls. The appropriate fluorophore-conjugated (Alexa 488 or Alexa 594, 1:2000) secondary antibodies (Jackson ImmunoResearch, West Grove, PA, USA) were used to reveal immune complexes. Afterward, the sections were rinsed for 10 min in PBST and either processed for a colabeling of primary and secondary antibodies or coverslipped under *Shur/Mount* mounting medium (Thermo Fisher). To avoid false-positive results attributable to cross-binding in double-label combinations, each primary antibody raised in a different species was used for double labeling. To stain the nuclei, 1.0 $\mu\text{g}/\text{ml}$ Hoechst33342 (Hoechst, Thermo Fisher) was added to the secondary antibody mixture. The immunostaining was examined, and images were captured using a Nikon TE2000-S fluorescence microscope (El Segundo, CA, USA) with filters suitable for selectively detecting the green, red, and blue fluorescence using a QuantiFire digital camera (Optronics, Ontario, NY, USA). For double labelling colocalization, images from the same specimen but showing different antigen signals were overlaid by digitally merging the captured images.

Quantification

Positive antibody immunostaining was defined as the cells having a fluorescence intensity greater than the average background fluorescence plus 2 standard deviations

of the cells in a section of negative control (the first antibody omitted) under identical acquisition parameters ($n = 10$ for different markers), identified by Hoechst counterstain at a different wavelength [31]. For quantification of GFP3.2iPA transduction efficiency, every fifth DRG section was selected from the consecutive serial sections (3 to 5 sections for each DRG), and in each selected section, the numbers of GFP labeled cells were counted and transduction efficiency was expressed as the percentage of total neuronal profiles revealed by b3-tubulin (Tubb3) staining [31].

Whole-cell current-clamp recording of dissociated DRG neurons

1. Dissociated DRG neuronal culture for electrophysiology was performed as described previously [20]. In brief, DRG (L4) from male rats were rapidly harvested from the isoflurane-anesthetized animals and were incubated in 0.01% liberate blendzyme 2 (Roche Diagnostics, Madison, WI) for 30 min, followed by incubation in 0.25% trypsin and 0.125% DNase for 30 min, both dissolved in DMEM/F12 with glutaMAX (Thermo Fisher). After exposure to 0.1% trypsin inhibitor and centrifugation, the pellet was gently triturated in a culture medium containing Neural basal media A (Thermo Fisher) plus 0.5 μM glutamine. Dissociated cells were plated onto 5% laminin-coated glass coverslips (Thermo Fisher), maintained at 37 °C in humidified 95% air and 5% CO_2 , and were studied in 6~8 h after harvest in electrophysiological experiments.
2. Whole-cell current-clamp recording of dissociated DRG neurons was performed as described previously [32], to determine the effects of AAV-mediated $\text{Ca}_v3.2\text{iPA2}$ expression on neuronal excitability. Dissociated small- and medium-sized DRG neurons (< 40 μm in diameter) from saline-injected animals and rats with MIA only, and dissociated DRG neurons with clear GFP expression from MIA rats injected with AAV6-NP or AAV6-3.2iPA2 at 6-week after vector injection were used for recording ($n = 5$ rats per group). For whole-cell current-clamp, patch electrodes had a resistance of 0.7–1.5 M Ω when filled with the pipette solution, which contained the following (in mM): 140 K-gluconate, 5 KCl, 2 MgCl₂, 0.2 EGTA, 10 HEPES, 4 Mg-ATP, and 0.3 Na²⁺-GTP, 10 Na₂-phosphocreatine pH 7.2 with KOH and osmolarity of 296 to 300 mOsm. The extracellular solution contained the following (in mM): 140 NaCl, 4 KCl, 2 CaCl₂, 2 MgCl₂, 10 D-glucose, 10 HEPES at pH of 7.4 with NaOH and an osmolarity of 300 mOsm. Whole-cell configuration was obtained in the volt-

age-clamp mode before proceeding to the current-clamp recording mode. The membrane input resistance was calculated by dividing the end amplitude of steady-state hyperpolarizing voltage deflection by the injected current [16, 33]. Action potentials (APs) were generated by injection of a series of current pulses (100 to 500 pA in steps of 100 pA, 250 ms). The baseline membrane potential had been recorded for 20 ms before the stimulus pulses were injected into the neurons. We defined the resting membrane potential (RMP) as the mean value of the 20 ms pre-stimulus membrane potential in the first trial and the AP rheobase as the minimum depolarizing current required to evoke the first AP. Given the knowledge that nerve injury induces high RMP and low rheobase in DRG neurons [34, 35], the neurons with stable RMP more negative than -45 mV and overshooting APs (> 80 mV RMP to peak) were used for additional data collection. AP frequency, an indicator of PSN excitability, was determined by quantifying the number of APs elicited in response to depolarizing current injections (250 ms).

Statistical analyses

All data are presented as mean \pm standard deviation of the mean (SEM) and were analyzed with GraphPad PRISM 9 (GraphPad Software, San Diego, CA, USA). The estimated numbers of animals needed for behavior were derived from our previous experience with similar experiments, and the statistical analyses were done afterward without interim data analysis [16]. No data points were excluded. $p < 0.05$ was considered statistically significant. Behavioral changes compared to pre-treatment baseline (BL) and between groups for von Frey, heat, and Wb measurements were generated using repeated measures two-way ANOVA and turkey post hoc for within-group analysis and Bonferroni test for between the groups. Pin and cold test results in discrete numerical data without normal distribution so conservative nonparametric analysis was performed by Friedman's tests and Dunn post hoc analysis. For comparisons between the groups, the effects of vector injection were characterized by the area under the curve (AUC) analysis. Specifically, the measured behavioral values after the combined injury and vector injection were normalized to the values immediately preceding injury and injection. For the evaluation of vector on established pain (in which vector injection was performed 14 days after nerve injury, BL), the measured values after the vector injection were normalized to the values immediately before the injection (treatment

baseline (tBL)) to calculate treatment AUC (tAUC). Calculated tAUCs were compared between vectors by Student's t test for von Frey, heat, and Wb and by Mann–Whitney U test pin and cold. The differences in the electrophysiological experiments were compared with one-way ANOVA, two-tailed unpaired t test, or Mann–Whitney test, where appropriate.

Results

MIA-induced knee damages shown in the current study were in accordance with those in our previous report [16]. MIA-treated knees in both male and female animals displayed typical structural joint damage, examined 56 days after MIA knee cavity injection. Knee injected with 2 mg of MIA showed a considerable loss of articular cartilage surrounding the subchondral bone along the joint, combined with reduced chondrocyte numbers, different degrees of bone marrow lesions, and collapse of subchondral bone (Fig. S1). The articular cartilage is incapable of directly generating pain because of both aneural and avascular. Thus, this study did not attempt to correlate MIA-induced cartilage loss, as well as other knee degeneration pathology, to pain behavior, and studies were focused on addressing whether a sensory neuron-selective block of T-type/Cav3.2 activity will mitigate neuropathic pain-like behavior.

Analgesia of established MIA-OA pain by DRG delivery of AAV6-3.2iPA2 in male rats

$\text{Ca}_v3.2\text{iPA2}$ (3.2iPA2) and $\text{Ca}_v3.2\text{iPA1}$ (3.2iPA1) are potent $\text{Ca}_v3.2$ inhibitory peptides derived from intrinsically disordered domains of Cav3.2 protein [20]. Our prior data showed that targeted DRG-PSN expression of AAV6-3.2iPA2 (and 3.2iPA1) was effective in the relief of pain behavior in a rat model of tibial nerve injury (TNI) neuropathic pain without affecting normal pain thresholds in naïve animals [20]. To broaden the testing of analgesic effects across different pain models, we set up experiments to address whether DRG delivery of AAV6-3.2iPAs is also effective in mitigating MIA-OA pain behavior. Specifically, the experiments were first aimed at testing whether AAV-mediated 3.2iPA2 expression selectively in the DRG-PSNs was effective in reversing the neuropathic pain-like behaviors, including evoked and spontaneous or ongoing pain, as well as weight-bearing asymmetry, following MIA knee injection. In the experimental design (Fig. 1A), the sensitivity to mechanical and thermal hindpaw cutaneous stimulation, as well as asymmetric hindlimb weight bearings on the injured limb loading, were assessed at baseline (before MIA) and weekly after MIA knee injection for 2 weeks before DRG delivery of AAV. After behavior tests at the 14th day following MIA, rats were randomized to receive

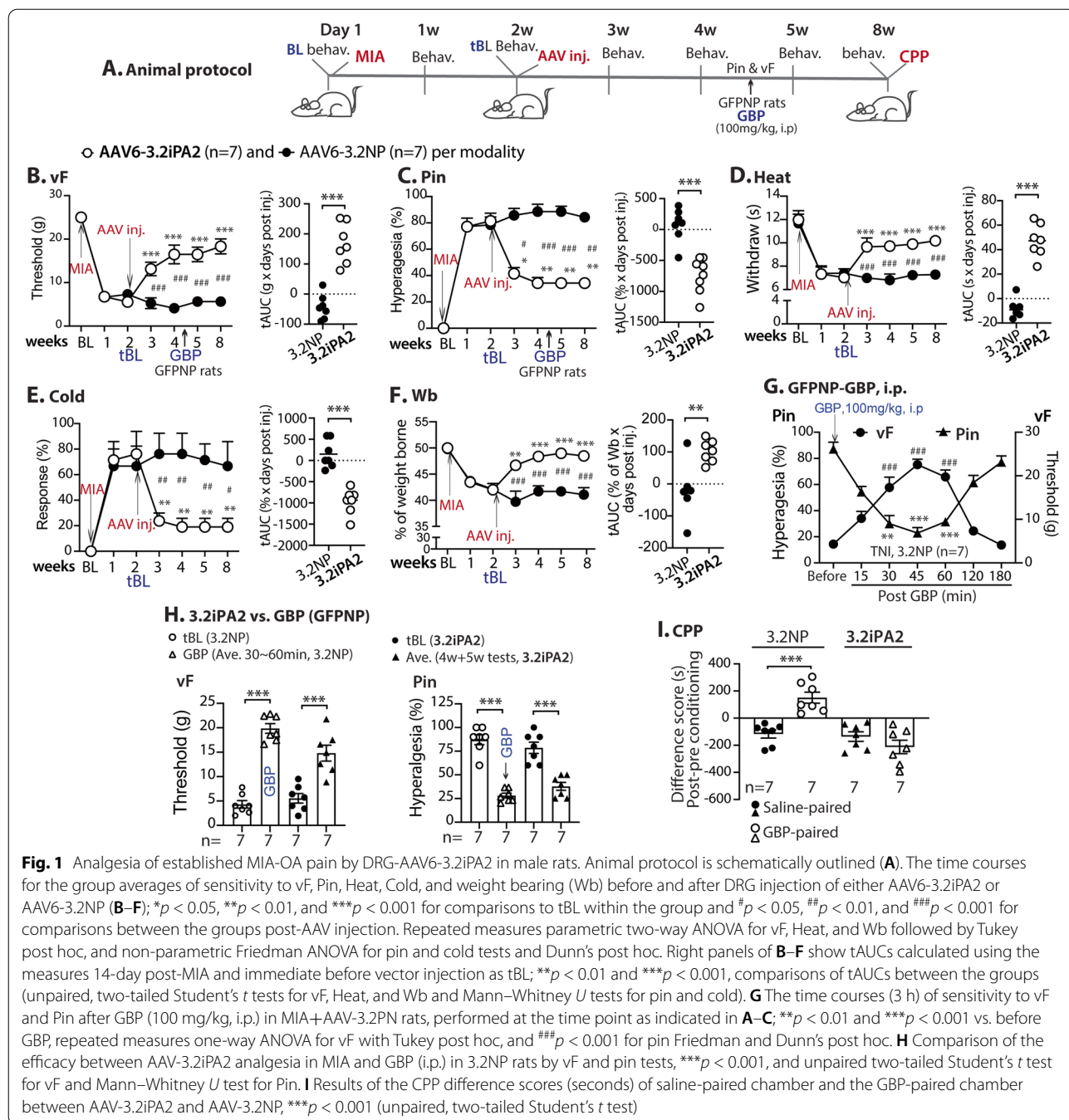


Fig. 1 Analgesia of established MIA-OA pain by DRG-AAV6-3.2iPA2 in male rats. Animal protocol is schematically outlined (A). The time courses for the group averages of sensitivity to vF, Pin, Heat, Cold, and weight bearing (Wb) before and after DRG injection of either AAV6-3.2iPA2 or AAV6-3.2NP (B-F); * $p < 0.05$, ** $p < 0.01$, and *** $p < 0.001$ for comparisons to tBL within the group and # $p < 0.05$, ## $p < 0.01$, and ### $p < 0.001$ for comparisons between the groups post-AAV injection. Repeated measures parametric two-way ANOVA for vF, Heat, and Wb followed by Tukey post hoc, and non-parametric Friedman ANOVA for pin and cold tests and Dunn's post hoc. Right panels of B-F show tAUCs calculated using the measures 14-day post-MIA and immediate before vector injection as tBL; ** $p < 0.01$ and *** $p < 0.001$, comparisons of tAUCs between the groups (unpaired, two-tailed Student's t tests for vF, Heat, and Wb and Mann-Whitney U tests for pin and cold). G The time courses (3 h) of sensitivity to vF and Pin after GBP (100 mg/kg, i.p.) in MIA+AAV-3.2NP rats, performed at the time point as indicated in A-C; ** $p < 0.01$ and *** $p < 0.001$ vs. before GBP, repeated measures one-way ANOVA for vF with Tukey post hoc, and ### $p < 0.001$ for pin Friedman and Dunn's post hoc. H Comparison of the efficacy between AAV-3.2iPA2 analgesia in MIA and GBP (i.p.) in 3.2NP rats by vF and pin tests, *** $p < 0.001$, and unpaired two-tailed Student's t test for vF and Mann-Whitney U test for Pin. I Results of the CPP difference scores (seconds) of saline-paired chamber and the GBP-paired chamber between AAV-3.2iPA2 and AAV-3.2NP, *** $p < 0.001$ (unpaired, two-tailed Student's t test)

intraganglionic injection of either AAV6-3.2iPA2 (treatment) or AAV6-3.2NP (control) into the ipsilateral L4/L5 DRG, since these DRG innervate knee and sciatic nerves, and show evidence of injury and increased T-type/Cav3.2 activity in knee MA-OA animals [16, 36]. Thereafter, sensory behavior evaluation was performed on a weekly basis for an additional 6 weeks. Single-dose GBP (100mg/kg, i.p.) was administered to the rats between the 4th and 5th weeks after AAV6-3.2NP vector (control)

injection as a positive control to compare antinociceptive effectiveness between the AAV6-3.2iPA2 treatment and GBP. The GBP-CPP test was performed in both AAV6-3.2iPA2 and AAV6-3.2NP groups after the observation course to evaluate spontaneous affective pain between the treatment and the control groups. The sensory behavior testing before vector injection at the 14th day after MIA knee injection was used to evaluate pain behavior development induced by MIA knee injection and also as

a treatment baseline (tBL) to compare the efficacy post vector injection. After which, the tissues were harvested for IHC characterization of transgene and target gene expression and for current-clamp recordings of PSN excitability.

The results showed that all rats received 2 mg MIA knee injection established significant ipsilateral pain behavior 2 weeks after MIA, tested on the plantar surface of the arthritic hindpaw, which included reduced threshold for withdrawals from mild mechanical stimuli (vF testing), more frequent hyperalgesic-type responses after noxious mechanical stimulation (pin testing), more frequent withdrawals to heat and cold stimuli (acetone stimulation), and increased arthritic hindlimb weight bearing asymmetry throughout the course of the study. These behaviors persisted in arthritic hind limbs after injection of the control AAV6-NP during the 6 weeks post-injection observation course. In contrast, MIA rats injected with AAV6-3.2iPA2 showed progressive and persistent reversal of these behavioral changes (Fig. 1B–F). Interestingly, MIA-induced changes in weight distribution in the arthritic hindpaw paralleled changes in hindpaw mechanical and thermal sensitivity, suggesting neuropathic components responsible for weight bearing asymmetry after 2 weeks of inflammation stage. GBP (i.p.) applied between the 4th and 5th weeks in MIA+AAV6-3.2NP rats substantially reversed mechanical hypersensitivity at 30 to 60 min after GBP, but animals were fully mechanically hypersensitive again 3 h after injection (Fig. 1G). The average (4w+5w) allodynia (vF) and hyperalgesia (Pin) in MIA+AAV6-3.2iPA2 group (~ 60% reversal of tBL) were comparable to the averaged (30 + 45min) values post-intraperitoneal administration of GBP in AAV6-GFPNP group (Fig. 1H). Spontaneous pain is a feature of knee MIA-OA pain, and CPP is the method of testing that has been shown to indicate the presence of spontaneous pain [37]. Using a biased CPP paradigm [38], the effect of AAV-3.2iPA2 treatment on spontaneous pain was evaluated. None of the animals in both groups was excluded from the study because of their extreme baseline preference/avoidance for a chamber [38]. A significant CPP effect was observed in the MIA rats injected with AAV6-3.2NP while there was no significant difference in the times spent in the initially nonpreferred chamber during baseline vs. test period in AAV-3.2iPA2-treated MIA animals (Fig. 1I). This indicates that MIA rats treated with AAV-3.2iPA2 relieved ongoing or spontaneous pain amenable to GBP treatment.

AAV-mediated $Ca_v3.2iPA2$ expression in vivo

The in vivo transduction rate for AAV6-3.2iPA2 6 weeks after vector injection was determined by IHC. The 3.2iPA2-positive neurons (GFP) comprised $41 \pm 10\%$

(824 out of 1986 total neuronal profiles), positive for pan-neuronal marker $\beta3$ -tubulin, $n = 3$ DRG, five sections per DRG, which were selected as every fifth section from the consecutive serial sections. Transduced DRG neurons included the full-size range of the PSNs that also expressed $Ca_v3.2$ (Fig. 2A–C), and GFP3.2iPA2 signals were not detected in the GFAP-positive DRG perineuronal glia cells (Fig. 2D).

Analgesia of DRG-AAV6-3.2iPA2 treatment in female MIA-OA rats

Sex differences exist in experimental and clinical pain and in response to pain interventions [39]. We therefore next tested whether DRG-AAV6-3.2iPA2 treatment is also effective in attenuating pain behavior and weight-bearing asymmetry induced by MIA knee injection in female animals, using the same animal protocol as that in male rats (Fig. 1A). Specifically, vector injection was performed 2 weeks after right knee MIA, both evoked mechanical and thermal nociception, arthritic limb weight-bearing asymmetry, and GBP-CPP were evaluated. The same batch preparation of AAV6-3.2iPA2 tested in the male rats was used. The results (Fig. 3A–E) showed that the female MIA-OA rats displayed comparable phenotypic development of hypersensitivity after induction of MIA-OA to male rats and that both evoked mechanical/thermal hypersensitivity, arthritic limb weight-bearing asymmetry, and GBP-CPP responses were substantially normalized after AAV6-3.2iPA2 treatment, showing analgesic effects comparable to those in male animals. IHC on the DRG sections from the female MIA rats 6 weeks after intraganglionic injection of AAV6-3.2iPA2 also revealed a comparable GFP-3.2iPA2 expressive profile to the male rats (Fig. 3F, not quantified). Thus, although male and female groups were not directly compared, a sexual dimorphism was not apparent for either pain behavior phenotypes after MIA or for the response to DRG-3.2iPA2 treatment in this study.

Together, these findings suggest that AAV6-mediated, DRG-targeted $Ca_v3.2iPA2$ treatment has analgesic efficacy in normalizing the established peripheral hypersensitivity displaying as evoked and spontaneous ongoing pain in a rat model of MIA-induced OA-pain, effective in both males and females. Additionally, the arthritic limb weight-bearing asymmetry was also significantly normalized. A sexual dimorphism seemed not apparent for both pain behavior phenotypes after MIA knee injection and in responsivity to DRG-3.2iPA2 treatment. Notably, sustained analgesic effectiveness was observed for several weeks during the testing course of this study. Sustained analgesic effectiveness will require evaluation in future studies.

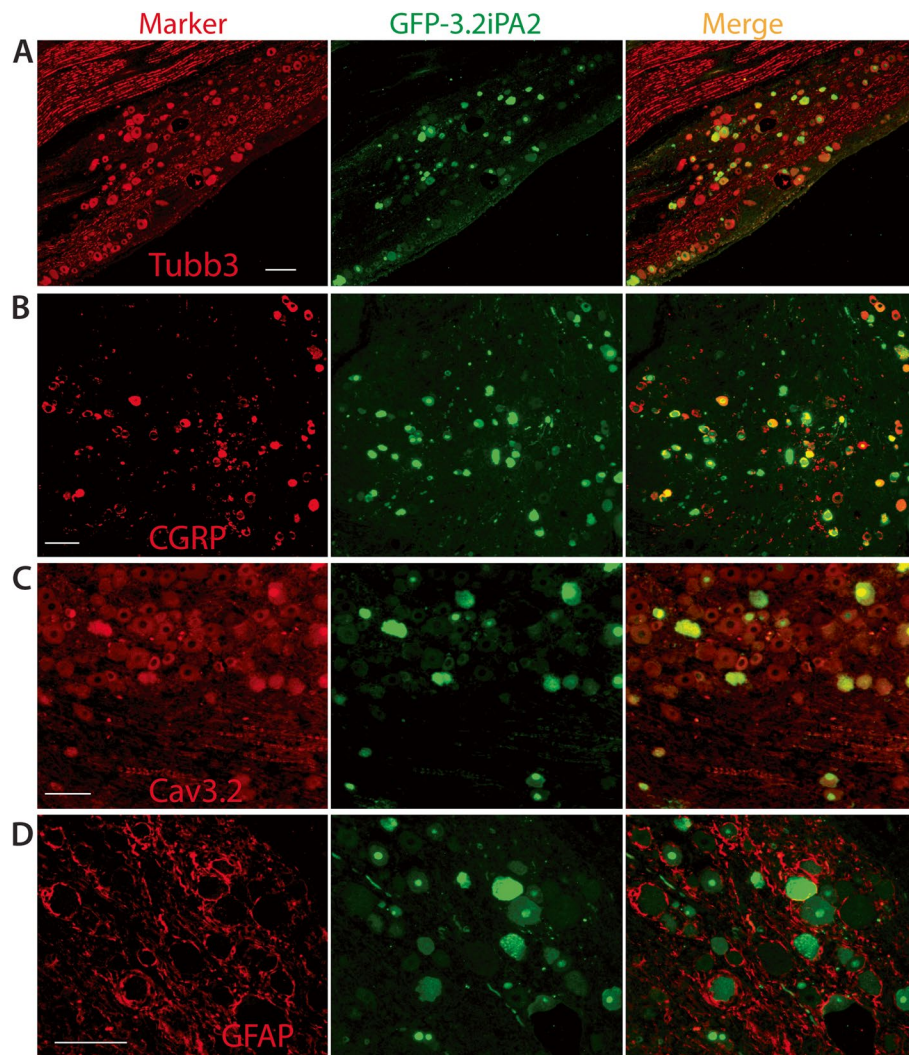


Fig. 2 IHC characterization of 3.2iPA2 expression in vivo (male). Representative IHC montage images show GFP-3.2iPA2 expression (green), colabeled with Tubb3 (A, red), CGRP (B, red), $Ca_v3.2$ (C, red), and GFAP (D, red). GFP-3.2iPA2 signal (green) is not detected in GFAP-positive glial cells (D, red). Scale bar, 100 μ m for all images

Reversal of MIA-induced PSN hyperexcitability of MIA-OA pain by AAV6- $Ca_v3.2iPA2$ treatment (male rats)

$Ca_v3.2$ channels contribute to nociception by driving burst firing of action potentials (AP) in PSNs, implying that activation of $Ca_v3.2$ channels could underlie OA pain-related increase in DRG-PSN hypersensitivity. Our previous study showed that $Ca_v3.2iPA$ attenuation of neuropathic pain in a TNI model is associated with reversal of injury-induced neuronal hypersensitivity [20]. Therefore, we next test whether analgesia of DRG-3.2iPA treatment in MIA-OA pain is associated with suppression of PSN hyperexcitability. Although MIA results in DRG with co-mingled injured and uninjured axons, nerve injury can induce an increase of voltage-gated ion

channel activity in both injured neurons and adjacent intact neurons, leading to similar electrophysiological changes and increased discharge frequency in damaged and neighboring intact DRG neurons [40]. We therefore recorded from randomly chosen small- and medium-sized neurons in the cultures from dissociated L4 DRG. Sensory neurons (small/medium, < 40 μ m in diameter) [41] dissociated from DRG of saline-injected rats and MIA rats without treatment, GFP-expressing neurons injected with either AAV6-GFPNP or AAV6-3.2iPA2, were used for recording. Transduced neurons were identified by GFP fluorescence, and excitability was evaluated by measuring the rheobase and the repetitive firing during 250-ms current injection steps. The effect

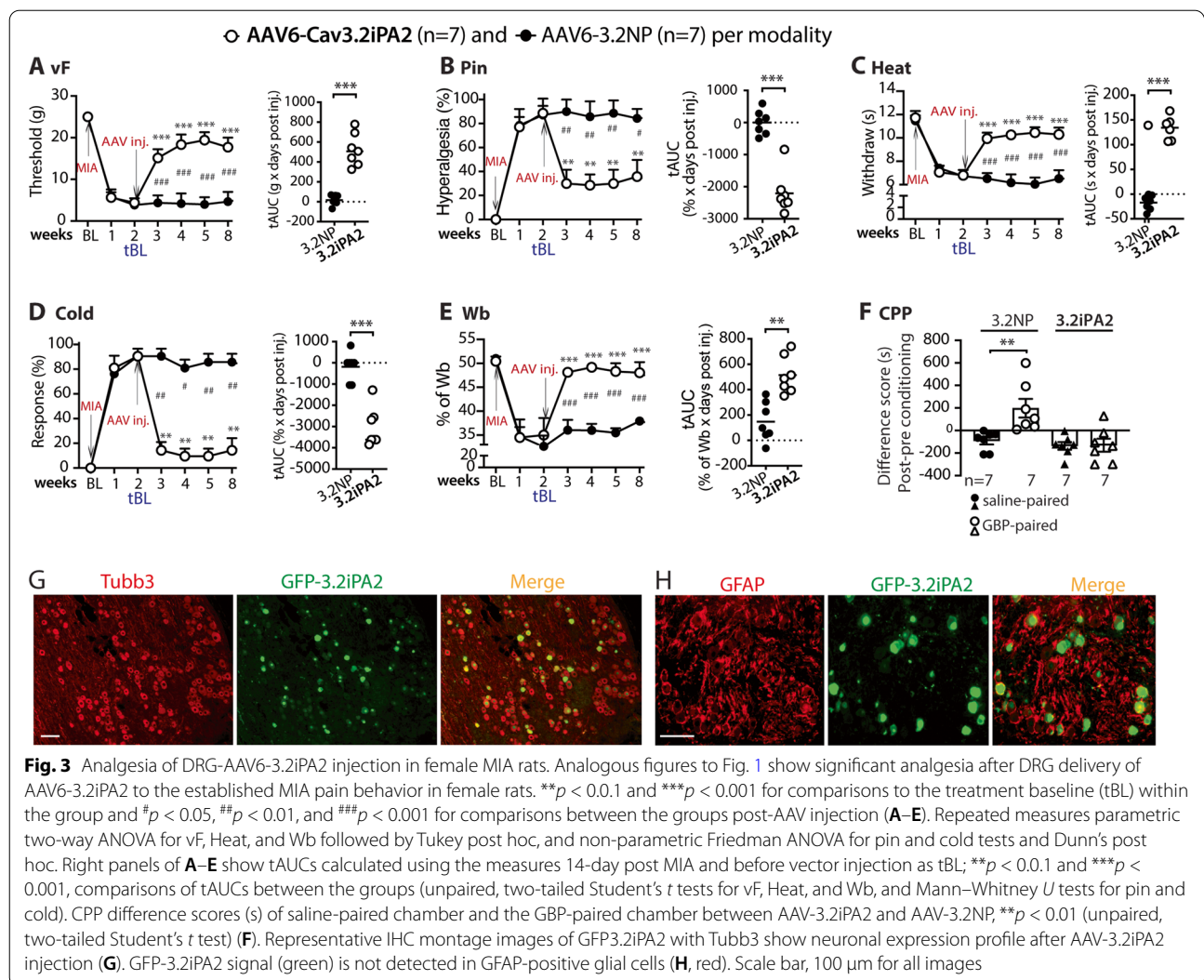
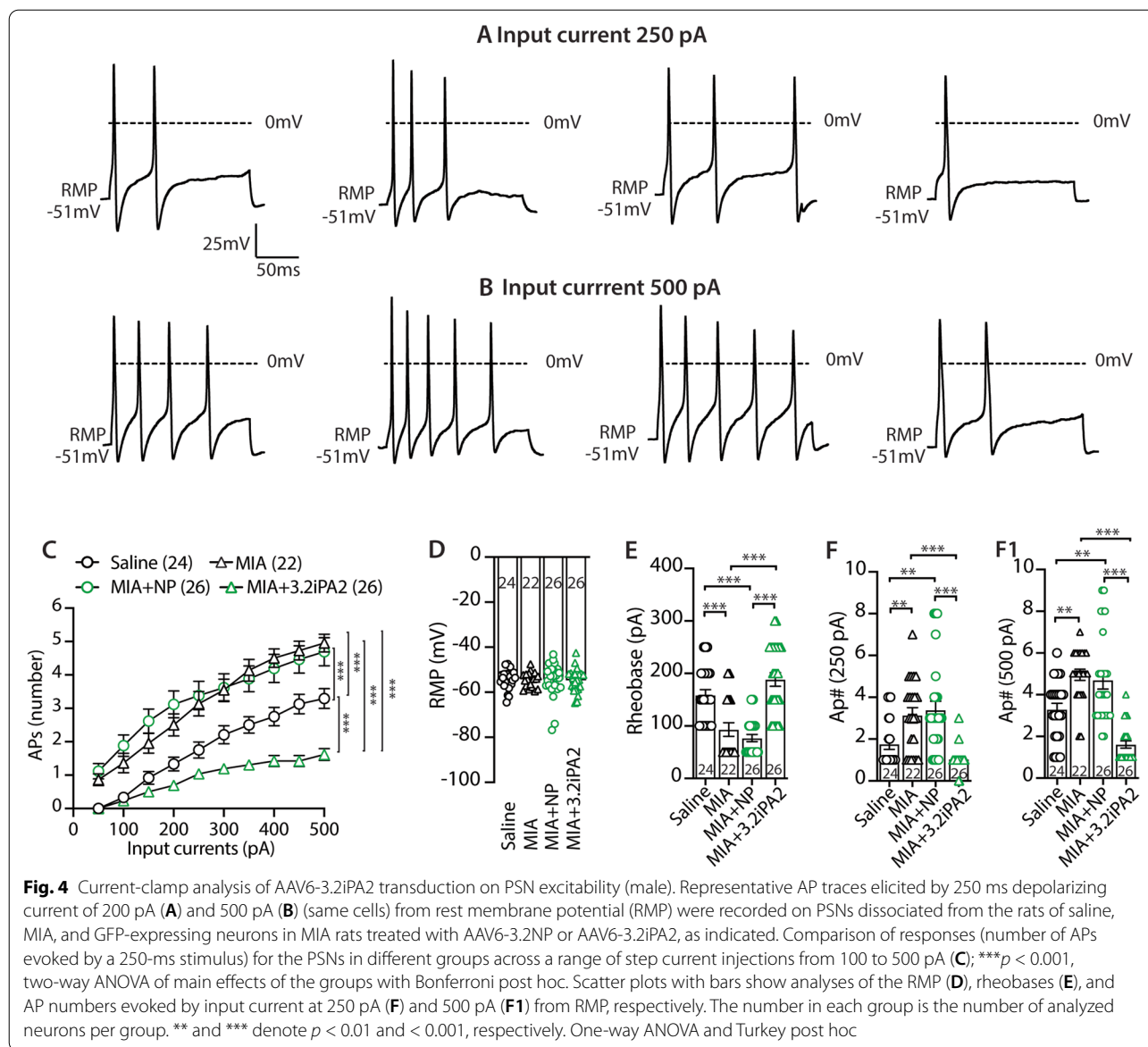


Fig. 3 Analgesia of DRG-AAV6-3.2iPA2 injection in female MIA rats. Analogous figures to Fig. 1 show significant analgesia after DRG delivery of AAV6-3.2iPA2 to the established MIA pain behavior in female rats. $**p < 0.01$ and $***p < 0.001$ for comparisons to the treatment baseline (tBL) within the group and $^{\#}p < 0.05$, $^{\#\#}p < 0.01$, and $^{\#\#\#}p < 0.001$ for comparisons between the groups post-AAV injection (A–E). Repeated measures parametric two-way ANOVA for vF, Heat, and Wb followed by Tukey post hoc, and non-parametric Friedman ANOVA for pin and cold tests and Dunn’s post hoc. Right panels of A–E show tAUCs calculated using the measures 14-day post MIA and before vector injection as tBL; $**p < 0.01$ and $***p < 0.001$, comparisons of tAUCs between the groups (unpaired, two-tailed Student’s *t* tests for vF, Heat, and Wb, and Mann–Whitney *U* tests for pin and cold). CPP difference scores (s) of saline-paired chamber and the GBP-paired chamber between AAV-3.2iPA2 and AAV-3.2NP, $**p < 0.01$ (unpaired, two-tailed Student’s *t* test) (F). Representative IHC montage images of GFP3.2iPA2 with Tubb3 show neuronal expression profile after AAV-3.2iPA2 injection (G). GFP-3.2iPA2 signal (green) is not detected in GFAP-positive glial cells (H, red). Scale bar, 100 μm for all images

of AAV6-3.2iPA2 expression on the DRG-PSN repetitive firing properties was assessed by applying a series of 250-ms current injections to the DRG dissociated neurons. Although RMP in the neurons from MIA did not differ from saline animals as reported previously [42], the frequency of APs evoked by progressively greater depolarizations in the recorded neurons from MIA rats was significantly increased, compared to saline controls, as previously reported [43]. The increased PSN excitability in MIA rats was normalized in the transduced neurons after AAV6-3.2iPA2 treatment, whereas AAV6-NP-transduced neurons had no effect (Fig. 4). Together, these findings indicate that the reversal of MIA-induced sensory neuronal hyperexcitability [16] by Cav3.2iPA2 may contribute to its attenuation of neuropathic pain behaviors.

Analgesia of DRG AAV6-3.2iPA1 treatment in MIA-OA rats in male rats

Analogous to the analgesic effects of AAV-3.2iPA2, DRG injection of AAV-3.2iPA1 resulted in a comparable effectiveness of pain relief against both evoked mechanical and thermal hypersensitivity, spontaneous pain behavior, and asymmetric hindlimb weight bearings (Suppl. Fig. 2). A similar in vivo transduction profile to AAV6-3.2iPA1 in male rats was observed for intraganglionic injection of AAV6-3.2iPA1 (not quantified). We did not test the effects of 3.2iPA1 on MIA-induced PSN hyperexcitability. However, reversal of MIA-induced PSN hyperexcitability by AAV6-3.2iPA1 treatment is expected, as we have shown in our previous report that 3.2iPA1 suppresses PSN hyperexcitability following TNI neuropathic pain [20].



Discussion

Our data affirm that AAV- $Ca_v3.2iPA$ mediated PSN-selective block of T-type/ $Ca_v3.2$ activity significantly mitigates evoked hindpaw hypersensitivity in knee MIA-OA rats. Moreover, the PSN-targeted block of T-type/ $Ca_v3.2$ channels normalizes the arthritic limb weight-bearing asymmetry and the aversiveness of ongoing pain (i.e., affective dimension of spontaneous pain). These data suggest that PSN injury in somata is a significant driver for MIA-OA pain. Dysfunction of T-type/ $Ca_v3.2$ seems to be a pathological requisite that contributes to the development and maintenance of neuropathic pain-like behavior in MIA-OA, and block of the firing of action potentials through inhibition of

T-type/ $Ca_v3.2$ in PSNs may be an effective means of mediating analgesia in MIA-OA. This is consistent to a previous report showing that DRG stimulation, which suppresses sensory neuronal excitability [44], alleviates pain behaviors in rat MIA-OA models [45]. Additionally, $Ca_v3.2iPA1/2$ inhibit both $Ca_v3.2$ and $Ca_v3.1$ currents (but not $Ca_v3.3$ current), demonstrated in our prior study [20]. Thus, the multipronged feature of $Ca_v3.2iPA1/2$ with combined $Ca_v3.2$ and $Ca_v3.1$ inhibition restricted to PSNs may provide an additional analgesic advantage because both are known nociceptive hubs [18, 46].

In OA, the early stage of pain generation of neuropathic components is conceivably initiated at the injury

side due to sensitized PSNs innervating joint, by which the specialized sensory afferents detect joint damage-derived chemical, mechanical, or thermal algogenic stimuli. This rationalizes the local intervention of sensitized sensory afferents, i.e., pain arising from the site of injury [47, 48]. However, recent advances have highlighted that pain-related sensory innervation in OA pain progressively induces morbidity in the PSN somata in addition to arthritis knee pathology [11]. DRG (and spinal cord) changes have been recently recognized to be associated with pain chronicity in OA, especially at the advanced stage of disease [49]. More recent literature has documented profound molecular and cellular changes in the DRG of various OA models, including changes in neuronal excitability [50], intense proliferation and activation of microglia that mediate neuroinflammation, and neuronal damage [15, 51–53], transcriptomic upregulation of the genes for neuroimmune interactions [54], sensitized PSN nociceptive voltage-gated ion channels [16, 55] and mechanosensitive ion channels [42], and upregulated chemokine and cytokine production [56], all contributing interrelatedly in driving continuous neural sensitization after cessation of joint inflammation.

Several mechanisms may determine that DRG-PSN morbidity in OA may not be limited exclusively to knee-innervating PSNs. Primarily, although PSN somata in DRG are anatomically isolated from each other and are not synaptically interconnected, most DRG-PSNs are transiently depolarized when axons of neighboring neurons of the same ganglion are stimulated repetitively [57]. This implicates that peripheral tissue inflammation and sensitization can induce DRG neuronal cross-depolarization coupling that adjacent neurons activate together contributing to pain hypersensitivity, but this rarely happens in naive animals [40]. And this coupling activation occurs among various sized neurons including small-diameter nociceptors and large-diameter low-threshold mechanoreceptors [40]. Therefore, although MIA produces DRG with co-mingled sensitized and “normal” axons, damaged neurons can induce an increase of pronociceptive ion channel activity in both damaged neurons and adjacent intact neurons, leading to similar electrophysiological changes and increased discharge frequency in the damaged and neighboring intact PSNs. Additionally, microglial mechanisms contribute to OA-pain as in neuropathic pain [58], and the activated microglia can sense and regulate neuronal activity, which is expected to affect all populations of PSNs, since the highly proliferated microglia can be detected in wrapping most of the PSNs in DRG ipsilateral to MIA injection [14, 16]. Together, PSNs in OA pain can be extensively hypersensitized and convert the sensitized signals into action

potentials, transmitted along PSN somata and afferents extending to peripheral terminals that decode dermatome sensitization and referred pain independent of joint damage, and to central terminals that relay the painful stimuli to the spinal DH and then to higher levels of the central nervous system neuraxis where they are decoded as conscious pain responses.

DRG-targeted pain interventions, such as DRG stimulation [44, 45] and pronociceptive molecule knock-out in PSNs [43, 59], have been proved to be effective in mitigating OA pain behavior. The success of these DRG-targeted interventions gives us the insight to rationalize that AAV-mediated block of PSN excitability can be an alternative approach to effectively mitigate OA pain behavior. Here, the results proved that AAV-mediated DRG-targeted block of sensory neuronal T-type/ $Ca_v3.2$ activity succeeded in attenuating neuropathic pain behavior in a rat model of MIA-OA pain. Small molecule inhibitors selective for $Ca_v3.2$ have been shown to produce dose-dependent antinociception in rat MIA-induced knee-joint pain [60] and neuropathic pain [61]. However, the widespread expression and multitude functional processes controlled by T-type/ $Ca_v3.2$ have complicated the use of blockers for chronic pain [62]. For clinical analgesia, the peripheral sensory nervous system (PSNS) is a particularly accessible site for devising new treatments, especially the DRG-PSNs which initiate nociception and have a central role in the development and maintenance of painful neuropathy [63]. Delivering drugs to the PSNS is well developed and safe, for instance, as used in clinical anesthesia for regional blockade and by pain physicians for diagnosis and treatment of radiculopathy [64]. Injection into the DRG has minimal consequences in preclinical models [22]. It has also been demonstrated that unintentional intraganglionic injection commonly accompanies clinical foraminal epidural steroid injection [64], a very common procedure with minimal risk of nerve damage. Thus, the PSNs are particularly suitable for targeting new analgesic treatments, especially at the level of the associated pathological DRG.

This study is formulated to test the effectiveness of targeting PSN-T-type/ $Ca_v3.2$ for OA-pain relief. A limitation is that a MIA-OA model is used in our current study, which can be differentiated in pain pathogenesis from human OA pain; however, features of MIA-induced disease is relevant to some aspects of human OA [65], including the knee damages and neuropathic pain-like symptoms. Additionally, whether DRG-targeted approach would prevent the nociceptive signals from reaching the SDH needs to be further investigated. One caveat of the present study is

that therapeutic AAV vector is selectively tropism to PSNs with minimal glial tropism. Given the increasing evidence that DRG reactive microgliosis play a critical role in the development of OA pain [14], microglia and related signaling molecules hold promise as targets for OA pain control. Ideally, the development of AAV vector that carries chimeric peptide aptamers or aptamer-siRNA chimeras capable of interfering with multiple dysfunctional nociceptive hubs, as well as activated microglia, may hold substantial value as a therapeutic strategy for relieving refractory OA chronic pain.

Conclusions

Our data provide preclinical relevance showing that suppression of T-type/ $Ca_v3.2$ channels selectively in the PSNs may be a potential approach to intervene in chronic OA pain behavior. It is necessary to validate the therapeutic potential of this strategy in other OA models in future investigations.

Abbreviations

OA: Osteoarthritis; MIA: Monosodium iodoacetate; DRG: Dorsal root ganglia; PSN: Primary sensory neuron; vF: von Frey; CPP: Conditioned place preference; GBP: Gabapentin; AAV: Recombinant adeno-associated viruses; Cav3.2: T-type calcium channel $3.2\alpha1H$; 3.2iPA: Cav3.2 inhibitory peptide aptamer; 3.2NP: Cav3.2 N-terminal inert peptide; GFP: Green fluorescent protein; AP: Action potential; RMP: Rest membrane potential.

Supplementary Information

The online version contains supplementary material available at <https://doi.org/10.1186/s13075-022-02856-0>.

Additional file 1: Figure S1. MIA OA knee histopathology. H&E stained sagittal section of saline-injected knees, showing full-depth normal cartilage and normal subchondral bone structure in male (A) and female (C). OA-like findings in the representative H&E-stained sagittal sections of knee 8 weeks after MIA (2mg) injection, showing articular cartilage loss (arrowheads), reduced chondrocyte numbers, subchondral bone collapse (arrows) in both male (B) and female (D). Scale bar: 500 μ m for all. **Figure S2.** Analgesia of MIA-OA pain by DRG delivery of AAV6-3.2iPA1 (male rats). Analogous figures (A-F) to Fig. 1 for treatment with AAV6-3.2iPA2 shows comparable effectiveness to MIA-OA pain likewise to AAV6-3.2iPA2. Representative IHC montage images show double immunostaining of Tubb3 (red) and GFP-3.2iPA1 (green) (G). GFP-3.2iPA1 signal (green) is not detected in GFAP-positive glial cells (H, red). Scale bar: 100 μ m for all images.

Acknowledgements

This research was supported by a grant from the National Institutes of Health grant R61NS116203 (HY and QH), an award of 2022 Dr. Ralph and Marian Falk Medical Research Trust, Bank of America, Private Bank (HY and QHH), and a Wisconsin Economic Development Corporation (WEDC, 2021) award (HY and QHH).

Authors' contributions

BIZ and SMS are equally contributing authors. Conceived, designed, and oversaw the experiments: HY. Performed the experiments: BIZ, SMS, XH, CSQ, FF, and HY. Analyzed the data: BIZ, SMS, and HY. Contributed reagents/materials/analysis tools: FF. Obtain funding: HY and QHH. Wrote the manuscript: HY. Revised the manuscript: HY and QHH. All authors reviewed the manuscript. The authors read and approved the final manuscript.

Availability of data and materials

All experimental data generated or analyzed in this study are either included in this article (and its supplementary information files) or will be made available upon reasonable request.

Declarations

Ethics approval and consent to participate

All animal experiments were performed with the approval of the Medical College of Wisconsin (MCW) Institutional Animal Care and Use Committee in accordance with the National Institutes of Health Guidelines for the Care and Use of Laboratory Animals. Experiments were performed within an Association for Assessment and Accreditation of Laboratory Animal Care (AAALAC)-accredited institute (MCW).

Consent for publication

Not applicable.

Competing interests

The authors declare that they have no competing interests.

Author details

¹Department of Anesthesiology, Medical College of Wisconsin, Milwaukee, WI 53226, USA. ²Department of Orthopedic Surgery, Affiliated Hospital of Qingdao University, Qingdao, China. ³Department of Pharmacology and Toxicology, Mississippi University Medical Center, Jackson, MS 39216, USA.

Received: 20 April 2022 Accepted: 29 June 2022

Published online: 16 July 2022

References

- Mapp PI, Sagar DR, Ashraf S, Burston JJ, Suri S, Chapman V, et al. Differences in structural and pain phenotypes in the sodium monoiodoacetate and meniscal transection models of osteoarthritis. *Osteoarthr Cartil.* 2013;21(9):1336–45.
- Fu K, Robbins SR, McDougall JJ. Osteoarthritis: the genesis of pain. *Rheumatology (Oxford).* 2018;57(suppl_4):iv43–50.
- Thakur M, Rahman W, Hobbs C, Dickenson AH, Bennett DL. Characterisation of a peripheral neuropathic component of the rat monoiodoacetate model of osteoarthritis. *PLoS One.* 2012;7(3):e33730.
- Syx D, Tran PB, Miller RE, Malfait AM. Peripheral mechanisms contributing to osteoarthritis pain. *Curr Rheumatol Rep.* 2018;20(2):9.
- Hunter DJ, McDougall JJ, Keefe FJ. The symptoms of osteoarthritis and the genesis of pain. *Med Clin North Am.* 2009;93(1):83–100 xi.
- Power JD, Perruccio AV, Gandhi R, Veillette C, Davey JR, Syed K, et al. Neuropathic pain in end-stage hip and knee osteoarthritis: differential associations with patient-reported pain at rest and pain on activity. *Osteoarthr Cartil.* 2018;26(3):363–9.
- French HP, Smart KM, Doyle F. Prevalence of neuropathic pain in knee or hip osteoarthritis: a systematic review and meta-analysis. *Semin Arthritis Rheum.* 2017;47(1):1–8.
- Zolio L, Lim KY, McKenzie JE, Yan MK, Estee M, Hussain SM, et al. Systematic review and meta-analysis of the prevalence of neuropathic-like pain and/or pain sensitization in people with knee and hip osteoarthritis. *Osteoarthr Cartil.* 2021;29(8):1096–116.
- Wylde V, Beswick A, Bruce J, Blom A, Howells N, Gooberman-Hill R. Chronic pain after total knee arthroplasty. *EFORT Open Rev.* 2018;3(8):461–70.
- Thakur M, Dickenson AH, Baron R. Osteoarthritis pain: nociceptive or neuropathic? *Nat Rev Rheumatol.* 2014;10(6):374–80.
- Orita S, Ishikawa T, Miyagi M, Ochiai N, Inoue G, Eguchi Y, et al. Pain-related sensory innervation in monoiodoacetate-induced osteoarthritis in rat knees that gradually develops neuronal injury in addition to inflammatory pain. *BMC Musculoskelet Disord.* 2011;12:134.
- Wu Q, Henry JL. Changes in Abeta non-nociceptive primary sensory neurons in a rat model of osteoarthritis pain. *Mol Pain.* 2010;6:37.
- Kelly S, Dunham JP, Murray F, Read S, Donaldson LF, Lawson SN. Spontaneous firing in C-fibers and increased mechanical sensitivity in

- A-fibers of knee joint-associated mechanoreceptive primary afferent neurones during MIA-induced osteoarthritis in the rat. *Osteoarthr Cartil.* 2012;20(4):305–13.
14. Raouf R, Martin Gil C, Lafeber F, de Visser H, Prado J, Versteeg S, et al. Dorsal root ganglia macrophages maintain osteoarthritis pain. *J Neurosci.* 2021;41(39):8249–61.
 15. Zhuo M, Wu G, Wu LJ. Neuronal and microglial mechanisms of neuropathic pain. *Mol Brain.* 2011;4:31.
 16. Shin SM, Cai Y, Itson-Zoske B, Qiu C, Hao X, Xiang H, et al. Enhanced T-type calcium channel 3.2 activity in sensory neurons contributes to neuropathic-like pain of monosodium iodoacetate-induced knee osteoarthritis. *Mol Pain.* 2020;16:1744806920963807.
 17. Schuelert N, McDougall JJ. Involvement of Nav 1.8 sodium ion channels in the transduction of mechanical pain in a rodent model of osteoarthritis. *Arthritis Res Ther.* 2012;14(1):R5.
 18. Bourinnet E, Francois A, Laffray S. T-type calcium channels in neuropathic pain. *Pain.* 2016;157(Suppl 1):S15–22.
 19. Srinivasan PP, Parajuli A, Price C, Wang L, Duncan RL, Kirn-Safran CB. Inhibition of T-type voltage sensitive calcium channel reduces load-induced OA in mice and suppresses the catabolic effect of bone mechanical stress on chondrocytes. *PLoS One.* 2015;10(5):e0127290.
 20. Shin SM, Lauzadis J, Itson-Zoske B, Cai Y, Fan F, Natarajan G, et al. Targeting intrinsically disordered regions facilitates discovery of CaV3.2 inhibitory peptides for AAV-mediated peripheral analgesia. *Pain.* 2022; PMID:35420557. <https://doi.org/10.1097/j.pain.0000000000002650>.
 21. Im HJ, Kim JS, Li X, Kotwal N, Sumner DR, van Wijnen AJ, et al. Alteration of sensory neurons and spinal response to an experimental osteoarthritis pain model. *Arthritis Rheum.* 2010;62(10):2995–3005.
 22. Fischer G, Kostic S, Nakai H, Park F, Sapunar D, Yu H, et al. Direct injection into the dorsal root ganglion: technical, behavioral, and histological observations. *J Neurosci Methods.* 2011;199(1):43–55.
 23. Bove SE, Calcaterra SL, Brooker RM, Huber CM, Guzman RE, Juneau PL, et al. Weight bearing as a measure of disease progression and efficacy of anti-inflammatory compounds in a model of monosodium iodoacetate-induced osteoarthritis. *Osteoarthr Cartil.* 2003;11(11):821–30.
 24. Chaplan SR, Bach FW, Pogrel JW, Chung JM, Yaksh TL. Quantitative assessment of tactile allodynia in the rat paw. *J Neurosci Methods.* 1994;53(1):55–63.
 25. Wu HE, Gemes G, Zoga V, Kawano T, Hogan QH. Learned avoidance from noxious mechanical stimulation but not threshold Semmes Weinstein filament stimulation after nerve injury in rats. *J Pain.* 2010;11(3):280–6.
 26. Pan B, Yu H, Park J, Yu YP, Luo ZD, Hogan QH. Painful nerve injury upregulates thrombospondin-4 expression in dorsal root ganglia. *J Neurosci Res.* 2015;93(3):443–53.
 27. Juarez-Salinas DL, Braz JM, Etlin A, Gee S, Sohal V, Basbaum AI. GABAergic cell transplants in the anterior cingulate cortex reduce neuropathic pain aversiveness. *Brain.* 2019;142(9):2655–69.
 28. Juarez-Salinas DL, Braz JM, Hamel KA, Basbaum AI. Pain relief by supraspinal gabapentin requires descending noradrenergic inhibitory controls. *Pain Rep.* 2018;3(4):e659.
 29. Prus AJ, James JR, Rosecrans JA: Conditioned place preference. In: *Methods of Behavior Analysis in Neuroscience*. Edited by nd, Buccafusco JJ. Boca Raton; 2009.
 30. Park HJ, Sandor K, McQueen J, Woller SA, Svensson CI, Corr M, et al. The effect of gabapentin and ketorolac on allodynia and conditioned place preference in antibody-induced inflammation. *Eur J Pain.* 2016;20(6):917–25.
 31. Yu H, Fischer G, Ferhatovic L, Fan F, Light AR, Weihsrauch D, et al. Intraganglionic AAV6 results in efficient and long-term gene transfer to peripheral sensory nervous system in adult rats. *PLoS One.* 2013;8(4):e61266.
 32. Shin SM, Lauzadis J, Itson-Zoske B, Cai YS, Fan F, G N, Kwok WM, Puopolo M, Hogan GH, H. Y. Targeting intrinsically disordered regions facilitates discovery of CaV3.2 inhibitory peptides for AAV-mediated peripheral analgesia. *PAIN* (accepted). 2022. <https://doi.org/10.1097/j.pain.0000000000002650>.
 33. Joksimovic SL, Joksimovic SM, Tesic V, Garcia-Caballero A, Feseha S, Zamponi GW, et al. Selective inhibition of CaV3.2 channels reverses hyperexcitability of peripheral nociceptors and alleviates postsurgical pain. *Sci Signal.* 2018;11(545).
 34. Cai W, Zhao Q, Shao J, Zhang J, Li L, Ren X, et al. MicroRNA-182 alleviates neuropathic pain by regulating Nav1.7 following spared nerve injury in rats. *Sci Rep.* 2018;8(1):16750.
 35. McCallum JB, Kwok WM, Sapunar D, Fuchs A, Hogan QH. Painful peripheral nerve injury decreases calcium current in axotomized sensory neurons. *Anesthesiology.* 2006;105(1):160–8.
 36. Ivanavicius SP, Ball AD, Heapy CG, Westwood FR, Murray F, Read SJ. Structural pathology in a rodent model of osteoarthritis is associated with neuropathic pain: increased expression of ATF-3 and pharmacological characterisation. *Pain.* 2007;128(3):272–82.
 37. Okun A, Liu P, Davis P, Ren J, Remeniuk B, Brion T, et al. Afferent drive elicits ongoing pain in a model of advanced osteoarthritis. *Pain.* 2012;153(4):924–33.
 38. Pan B, Yu H, Fischer GJ, Kramer JM, Hogan QH. Dorsal root ganglionic field stimulation relieves spontaneous and induced neuropathic pain in rats. *J Pain.* 2016;17(12):1349–58.
 39. Mogil JS. Sex differences in pain and pain inhibition: multiple explanations of a controversial phenomenon. *Nat Rev Neurosci.* 2012;13(12):859–66.
 40. Kim YS, Anderson M, Park K, Zheng Q, Agarwal A, Gong C, et al. Coupled activation of primary sensory neurons contributes to chronic pain. *Neuron.* 2016;91(5):1085–96.
 41. Shin SM, Itson-Zoske B, Cai Y, Qiu C, Pan B, Stucky CL, et al. Satellite glial cells in sensory ganglia express functional transient receptor potential ankyrin 1 that is sensitized in neuropathic and inflammatory pain. *Mol Pain.* 2020;16:1744806920925425.
 42. He BH, Christin M, Mouchbahani-Constance S, Davidova A, Sharif-Naeini R. Mechanosensitive ion channels in articular nociceptors drive mechanical allodynia in osteoarthritis. *Osteoarthr Cartil.* 2017;25(12):2091–9.
 43. Soga M, Izumi T, Nanchi I, Horita N, Yamamoto M, Kawasaki S, et al. Suppression of joint pain in transient receptor potential vanilloid 4 knockout rats with monoiodoacetate-induced osteoarthritis. *Pain Rep.* 2021;6(3):e951.
 44. Koopmeiners AS, Mueller S, Kramer J, Hogan QH. Effect of electrical field stimulation on dorsal root ganglion neuronal function. *Neuromodulation.* 2013;16(4):304–11 discussion 310–301.
 45. Yu G, Segel I, Zhang Z, Hogan QH, Pan B. Dorsal root ganglion stimulation alleviates pain-related behaviors in rats with nerve injury and osteoarthritis. *Anesthesiology.* 2020;133(2):408–25.
 46. Na HS, Choi S, Kim J, Park J, Shin HS. Attenuated neuropathic pain in Cav3.1 null mice. *Mol Cell.* 2008;25(2):242–6.
 47. Kidd BL. Osteoarthritis and joint pain. *Pain.* 2006;123(1–2):6–9.
 48. Alves CJ, Couto M, Sousa DM, Magalhaes A, Neto E, Leitao L, et al. Nociceptive mechanisms driving pain in a post-traumatic osteoarthritis mouse model. *Sci Rep.* 2020;10(1):15271.
 49. Haywood AR, Hathway GJ, Chapman V. Differential contributions of peripheral and central mechanisms to pain in a rodent model of osteoarthritis. *Sci Rep.* 2018;8(1):7122.
 50. Qu L, Caterina MJ. Enhanced excitability and suppression of A-type K(+) currents in joint sensory neurons in a murine model of antigen-induced arthritis. *Sci Rep.* 2016;6:28899.
 51. Kwok CHT, Kohro Y, Mousseau M, O'Brien MS, Matyas JR, McDougall JJ, et al. Role of primary afferents in arthritis induced spinal microglial reactivity. *Front Immunol.* 2021;12:626884.
 52. Mousseau M, Burma NE, Lee KY, Leduc-Pessah H, Kwok CHT, Reid AR, et al. Microglial pannexin-1 channel activation is a spinal determinant of joint pain. *Sci Adv.* 2018;4(8):eaas9846.
 53. Tran PB, Miller RE, Ishihara S, Miller RJ, Malfait AM. Spinal microglial activation in a murine surgical model of knee osteoarthritis. *Osteoarthr Cartil.* 2017;25(5):718–26.
 54. Miller RE, Tran PB, Ishihara S, Syx D, Ren D, Miller RJ, et al. Microarray analyses of the dorsal root ganglia support a role for innate neuro-immune pathways in persistent pain in experimental osteoarthritis. *Osteoarthr Cartil.* 2020;28(5):581–92.
 55. Rahman W, Dickenson AH. Osteoarthritis-dependent changes in antinociceptive action of Nav1.7 and Nav1.8 sodium channel blockers: an in vivo electrophysiological study in the rat. *Neuroscience.* 2015;295:103–16.
 56. Goncalves WA, Rezende BM, de Oliveira MPE, Ribeiro LS, Fattori V, da Silva WN, et al. Sensory ganglia-specific TNF expression is associated with persistent nociception after resolution of inflammation. *Front Immunol.* 2019;10:3120.

57. Amir R, Devor M. Chemically mediated cross-excitation in rat dorsal root ganglia. *J Neurosci*. 1996;16(15):4733–41.
58. Geraghty T, Winter DR, Miller RJ, Miller RE, Malfait AM. Neuroimmune interactions and osteoarthritis pain: focus on macrophages. *Pain Rep*. 2021;6(1):e892.
59. Obeidat AM, Wood MJ, Ishihara S, Li J, Wang L, Ren D, et al. Piezo2 expressing nociceptors mediate mechanical sensitization in experimental osteoarthritis. *bioRxiv*. 2022. <https://doi.org/10.1101/2022.03.12.484097>.
60. Wallace M, Duan R, Liu W, Locke C, Nothaft W. A randomized, double-blind, placebo-controlled, crossover study of the T-type calcium channel blocker ABT-639 in an intradermal capsaicin experimental pain model in healthy adults. *Pain Med*. 2016;17(3):551–60.
61. Kerckhove N, Pereira B, Soriot-Thomas S, Alchaar H, Deleens R, Hieng VS, et al. Efficacy and safety of a T-type calcium channel blocker in patients with neuropathic pain: a proof-of-concept, randomized, double-blind and controlled trial. *Eur J Pain*. 2018;22(7):1321–30.
62. Patel R, Montagut-Bordas C, Dickenson AH. Calcium channel modulation as a target in chronic pain control. *Br J Pharmacol*. 2018;175(12):2173–84.
63. Hogan QH. Labat lecture: the primary sensory neuron: where it is, what it does, and why it matters. *Reg Anesth Pain Med*. 2010;35(3):306–11.
64. Pfirrmann CW, Oberholzer PA, Zanetti M, Boos N, Trudell DJ, Resnick D, et al. Selective nerve root blocks for the treatment of sciatica: evaluation of injection site and effectiveness—a study with patients and cadavers. *Radiology*. 2001;221(3):704–11.
65. Pomonis JD, Boulet JM, Gottshall SL, Phillips S, Sellers R, Bunton T, et al. Development and pharmacological characterization of a rat model of osteoarthritis pain. *Pain*. 2005;114(3):339–46.

Publisher's Note

Springer Nature remains neutral with regard to jurisdictional claims in published maps and institutional affiliations.

Ready to submit your research? Choose BMC and benefit from:

- fast, convenient online submission
- thorough peer review by experienced researchers in your field
- rapid publication on acceptance
- support for research data, including large and complex data types
- gold Open Access which fosters wider collaboration and increased citations
- maximum visibility for your research: over 100M website views per year

At BMC, research is always in progress.

Learn more biomedcentral.com/submissions

